PAPER

Discrete spacetime: a web of chains

IOP Publishing Classical and Quantum Gravity

Class. Quantum Grav. **36** (2019) 185015 (28pp) https://doi.org/10.1088/1361-6382/ab30e3

Discrete spacetime: a web of chains

M Aghili, L Bombelli and B B Pilgrim

Department of Physics and Astronomy, The University of Mississippi, University, MS 38677-1848

E-mail: maghili@go.olemiss.edu, bombelli@olemiss.edu and bbpilgri@go.olemiss.edu

Received 31 January 2019, revised 17 June 2019
Accepted for publication 10 July 2019
Published 28 August 2019

Abstract

This paper is a contribution to the study of the relationship between causal sets and Lorentzian manifolds. Given a causal set and a local region in it, identified with the interval between two elements, we use the distributions of chain and maximal-chain lengths in that region as a tool for establishing to what extent the region is manifoldlike. We first derive the mean length distributions for causal sets obtained from uniformly random sets of points in Minkowski space, in a form suitable to addressing our question. We then compare those distributions with the ones obtained from some examples of non-manifoldlike causal sets and, for manifoldlike causal sets, we compare some dimension estimators derived from the length distributions with other available dimension estimators.

Keywords: causal set theory, quantum gravity, discrete spacetime

(Some figures may appear in colour only in the online journal)

1. Introduction

Causal set theory is an approach to quantum gravity in which the continuum model of spacetime as a Lorentzian manifold is replaced by a locally finite partially ordered set, a set $\mathcal{C}$ with a binary relation $\prec$ which is (i) irreflexive[1] ($\forall p \in \mathcal{C},\ p \not\prec p$), (ii) transitive ($\forall p, q, r \in \mathcal{C},\ p \prec q \prec r \Rightarrow p \prec r$), and (iii) locally finite ($\forall p, q \in \mathcal{C}$, the cardinality of the *interval* $I(p, q) := \{r \mid p \prec r \prec q\}$ is finite). We interpret the relation $p \prec q$ as a causal structure on $\mathcal{C}$, the discrete analog of the chronology relation $x \in I^-(y)$ on a spacetime manifold $(\mathcal{M}, g)$, and the interval is then the discrete analog of an *Alexandrov set* or 'causal diamond' $A(x, y) := I^+(x) \cap I^-(y)$ in the continuum; here, the chronological future/past $I^{\pm}(y)$ of

[1] Partial orders are often defined as reflexive relations, such that $p \prec p$ for all $p \in \mathcal{C}$, satisfying the additional anti-symmetry condition that $p \prec q \Rightarrow q \not\prec p$ for all $p, q \in \mathcal{C}$. Each reflexive order corresponds to a unique irreflexive one, and vice versa.

$y \in \mathcal{M}$ is the set of points that can be reached by a future/past directed timelike curve from y, respectively, and the relation $x \in I^-(y)$ is a partial order if the spacetime has a well-behaved causal structure.

A (large) causal set $\mathcal{C}$ and a Lorentzian manifold $(\mathcal{M}, g)$ are seen as good approximations of each other if $\mathcal{C}$ can be faithfully embedded in $\mathcal{M}$ [1], which for the purposes of this paper can be taken to mean that there is a embedding $f : \mathcal{C} \to \mathcal{M}$ under which the elements of $\mathcal{C}$ are distributed with uniform density in $\mathcal{M}$ and the partial orders agree in the sense that $p \prec q$ iff $f(p) \in I^-(f(q))$. The uniform density condition is necessary, at least in flat spacetime, to ensure that the embedding process does not introduce a preferred frame or other additional structure in $\mathcal{M}$. This paper discusses criteria for establishing how manifoldlike a causal set is in this sense. We will focus on the case where $\mathcal{M}$ is Minkowski spacetime, which is of interest both as a simple spacetime in its own right and as a starting point for the study of more general causal sets, since in sufficiently small local regions they are approximately flat.

Let us define a few other terms to be used throughout this paper. A *chain* is a subset of $\mathcal{C}$ all of whose elements are pairwise related; in other words, a k-chain is a totally ordered set of the form $\{p_0, p_1, \ldots, p_k \mid p_0 \prec p_1 \prec \cdots \prec p_k\}$. Two elements of $\mathcal{C}$ are *linked* if they are related with no elements between them; we will denote this by the relation $p \prec\!\!* \, q :\Leftrightarrow (p \prec q) \;\&\; (I(p,q) = \emptyset)$. A *path* is a maximal chain, i.e. one which cannot be lengthened by including a new element of $\mathcal{C}$ between any two of its elements; a k-path is then a set of the form $\{p_0, p_1, \ldots, p_k \mid p_0 \prec\!\!* \, p_1 \prec\!\!* \cdots \prec\!\!* \, p_k\}$.

In a previous paper [2] we showed how to calculate the path length distribution (the mean number of k-paths as a function of k) for N-element causal sets obtained from uniformly random distributions of points inside an Alexandrov set $A(x, y)$ in 2D Minkowski space. Using that distribution and the results of numerical simulations we argued that the mean path length and width of the distribution provide a good criterion of embeddability of a causal set in flat spacetime. This paper extends those results in various ways. In section 2 we calculate the chain length distribution for causal sets uniformly embedded in d-dimensional Minkowski space. Importantly, we point out that to consistently address the question of the embeddability of a given causal set in flat space we need to modify the calculation of the chain length and path length distributions, which leads to somewhat different theoretical mean distributions. In section 3 we revisit and modify our results from [2], and extend them to d dimensions. In section 4 we return to the question of manifoldlikeness of causal sets, for which in the case of chains we can also calculate analytically the width of the length distribution. These results show the usefulness of these length distributions for the analysis of causal sets, and in section 5 we compare the results obtained using these and other methods when estimating the dimensionality of a flat spacetime in which a causal set can be embedded.

2. Chain length distributions in Minkowski space

In this section we develop an approach to determining how manifoldlike a local region in a causal set is, where the local region is identified with the interval $I(p, q)$ between two elements, based on comparing the number of k-chains c_k between p and q, for all k, with the expected values for a suitable ensemble of causal sets embedded in flat spacetime. (This may include the possibility of using the entire causal set as the 'local region' since formally, as long as its cardinality N is finite, we can add minimal and maximal elements p_0 and p_{N+1} to it and view it as the interval $I(p_0, p_{N+1})$.) If we use all of Minkowski space as the overall reference manifold, in order to avoid introducing any extra structure in it the natural choice for the comparison is to use subsets of the causal sets obtained from a Poisson point process in

Minkowski space $\mathcal{M}$. This produces independent, uniformly distributed ('sprinkled') random sets of points with some density ρ, characterized by the fact that the probability that any (measurable) region $R \subset \mathcal{M}$ contains n points is given by the Poisson distribution of mean ρV_R,

$$P(n) = \frac{\mathrm{e}^{-\rho V_R}\,(\rho V_R)^n}{n!},$$

where $V_R = \int_R \mathrm{d}V$ is the volume of R, with $\mathrm{d}V = \sqrt{-g(x)}\,\mathrm{d}^d x$ in d dimensions.

Let us denote by $\mathcal{C}$ the local region of interest within the overall causal set, considered as an N-element causal set in its own right. What specific subsets of causal sets sprinkled in Minkowski space should we compare $\mathcal{C}$ to? Two choices appear to be natural, (i) the ensemble of all subsets contained inside some fixed Alexandrov set $A(x, y)$ of volume $V = N/\rho$, or (ii) the ensemble of all N-element subsets contained in the Alexandrov set between any fixed pair of points x, $y \in \mathcal{M}$. In the first case it does not matter which such Alexandrov set we use, since the sprinkling process is Lorentz-invariant [3]; in the second case it does not matter which (x, y) we use, because of Lorentz invariance and because in this case the scale is set by N, an intrinsic property of the causal set, and no manifold scale or density need be mentioned. These two choices lead to somewhat similar but inequivalent results.

We take the point of view that option (ii) is more natural. Our motivation comes from the fact that it leads to a more intrinsic manifoldlikeness criterion, which can be stated without referring to any manifold scale or in fact making any assumption about the size of the overall reference spacetime. With option (i) we would be comparing $\mathcal{C}$ with subsets of an overall causal set that must be infinite for the Poisson distribution to be exact, while option (ii) can be stated with no implicit reference to the size of the overall causal set $\mathcal{C}$ is in or any property of the overall reference manifold, other than the flatness of the local region (in the context of this paper). We will therefore evaluate the extent to which a causal set $\mathcal{C}$ is manifoldlike by comparing c_k with the theoretical mean chain length distribution $\langle c_k \rangle$ for all intervals of size N in causal sets randomly sprinkled in some (causally convex) region of Minkowski space.

Let us now derive this mean chain length distribution $\langle c_k \rangle$. Since we can use any overall manifold region as long as it contains the Alexandrov set $A(x, y)$, in the theoretical derivation we will use this set itself; we will call it A_0 and its volume V_0. Then, for each point sprinkled uniformly inside A_0 the probability that it falls within or outside a region $R \subset A_0$ is V_R/V_0 or $(1 - V_R/V_0)$, respectively, and when N points are chosen uniformly at random the probability of finding exactly n of them inside R is given by the binomial distribution

$$P(n) = \binom{N}{n} \left(\frac{V_R}{V_0}\right)^n \left(1 - \frac{V_R}{V_0}\right)^{N-n}.$$

For example, in an infinitesimal volume $\mathrm{d}V$ the probability of finding a single point is $\mathrm{d}P = \rho\,\mathrm{d}V$, while the probability of finding $n > 1$ points is a higher-order differential.

In the causal set $\mathcal{C} = I(p, q)$, c_k counts chains of the form $p = p_0 \prec p_1 \prec \cdots \prec p_{k-1} \prec p_k = q$, so in the Alexandrov set $A_0 = A(x,y)$ the chains we will count are of the form $x = x_0 \prec x_1 \prec \cdots \prec x_{k-1} \prec x_k = y$. Their mean total number can be obtained by calculating the mean number of k-chains through $k - 1$ points x_i within a set of infinitesimal volumes $\{\mathrm{d}V_i\}$, with $x_i \in A(x_{i-1}, x_{i+1})$ for each $i = 1, ..., k - 1$, and integrating over those $k - 1$ locations. For each particular set of locations the probability of finding a k-chain from x_0 to x_{N+1} through them can be calculated by induction as follows. For $k = 1$ the probability is 1, and for $k = 2$ and 3 it is

$$\mathrm{d}P_{(2)}(x_1) = \rho_0\,\mathrm{d}V_1 = \frac{N}{V_0}\sqrt{-g(x_1)}\,\mathrm{d}^d x, \tag{1}$$

$$\mathrm{d}P_{(3)}(x_1,x_2) = \mathrm{d}P_{(2)}(x_1)\,\rho_1\,\mathrm{d}V_2 = \frac{N(N-1)}{V_0^2}\,\mathrm{d}V_1\,\mathrm{d}V_2, \tag{2}$$

provided that $x_2 \in I^+(x_1)$, where $\rho_0 = \rho = N/V_0$ and $\rho_1 = (N-1)/V_0$ is the effective density with which the remaining points are distributed given that one point is located at x_1 and there are only $N-1$ points left to locate; the fact that these densities do not have the same value is important and we will comment on its consequences below. Similarly, for each other k the probability is obtained from the recursion relation

$$\mathrm{d}P_{(k)}(x_1,...,x_{k-1}) = \mathrm{d}P_{(k-1)}(x_1,...,x_{k-2})\,\rho_{k-2}\,\mathrm{d}V_{k-1}, \tag{3}$$

where $\rho_i = (N-i)/V_0$ for all i. The expected number of k-chains from x_0 to x_{N+1} through the $\{\mathrm{d}V_i\}$ is then the sum

$$\mathrm{d}\langle c_k(x_1,...,x_{k-1})\rangle = \sum_{n=0}^{n_{\max}} n\cdot(\text{probability of } n \text{ chains through the } \{\mathrm{d}V_i\}) \tag{4}$$

over possible values of the number n of k-chains. The term with $n=0$ clearly does not contribute to the sum, while the terms with $n>1$ are higher-order differentials, so we are left with

$$\mathrm{d}\langle c_k(x_1,...,x_{k-1})\rangle = \mathrm{d}P_{(k)}(x_1,...,x_{k-1}). \tag{5}$$

In words, the expected number of k-chains coincides with the probability that there is one chain through the $k-1$ differential volumes. We can therefore find the mean total number $\langle c_k\rangle$ of k-chains from x_0 to x_{N+1} by integrating this expression over all the x_i, with each point in the future of the previous one, $x_i \in I^+(x_{i-1})$,

$$\begin{aligned}\langle c_k\rangle &= \int_{A_0}\rho_0\,\mathrm{d}V_1\int_{A_1}\rho_1\,\mathrm{d}V_2\cdots\int_{A_{k-2}}\rho_{k-2}\,\mathrm{d}V_{k-1},\\ &= \frac{N(N-1)(N-2)\cdots(N-(k-2))}{V^{k-1}}\int_{A_0}\mathrm{d}V_1\int_{A_1}\mathrm{d}V_2\cdots\int_{A_{k-2}}\mathrm{d}V_{k-1},\end{aligned} \tag{6}$$

where A_i is short for $A(x_i,x_k)$. A guide to the eye is provided in figure 1, where for a k-chain we are identifying $x_k = x_{N+1}$. After integrating and rewriting the coefficient, in Minkowski space this expression simplifies to

$$\langle c_k\rangle = \frac{N!}{(N-(k-1))!}\left(\frac{\Gamma(d+1)}{2}\right)^{k-2}\frac{\Gamma(d/2+1)\,\Gamma(d)}{\Gamma((k-1)d/2+1)\,\Gamma(kd/2)}, \tag{7}$$

for all positive k; in particular, notice that $\langle c_k\rangle = 0$ for $k > N+1$.

We should emphasize the fact that the effective densities ρ_i are not all equal to each other; this is because of our choice to consider the ensemble of only N-element causal sets embedded in the Alexandrov set A_0. In the previous literature, though not explicitly stated, the authors implicitly made the choice of replacing N with Poisson-distributed values of n by assuming that $\rho_i = \rho_0$ (this includes our own work [2], as well as references in which this assumption was hidden by the use of units in which $\rho = 1$ [4]), in which case instead of equation (7) one gets the following chain length distribution, again valid for all positive k, which only vanishes in the $k\to\infty$ limit:

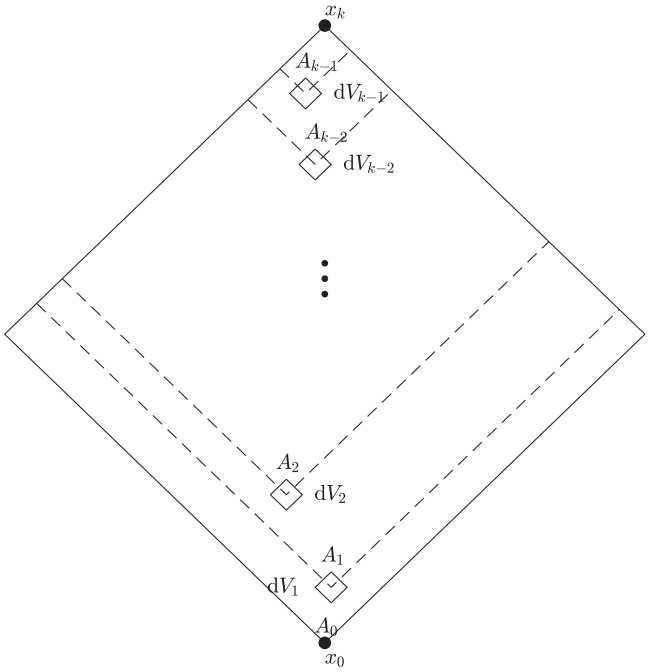

Figure 1. A visual representation of the volumes involved in the calculation of the expected number of chains $\langle c_k \rangle$ of length k in a causal set obtained from points uniformly distributed inside an Alexandrov set in Minkowski spacetime.

$$\langle c_k \rangle_0 = N^{k-1} \left(\frac{\Gamma(d+1)}{2} \right)^{k-2} \frac{\Gamma(d/2+1)\,\Gamma(d)}{\Gamma((k-1)d/2+1)\,\Gamma(kd/2)}. \tag{8}$$

(For comparison with [4], we point out that our k-chains are called $(k+1)$-chains there, and our d is the full spacetime dimension.) The difference between the values obtained using the two distributions (7) and (8) can be seen by comparing figures 2 and 3. The former shows the results of $m = 10\,000$ sprinkled causal sets with $N = 100$ in Minkowski space of various dimensionalities together with the theoretical distributions from equation (8) for $N = 100$, while in the latter figure the distribution in equation (7) is used with the same set of random causal sets. The exact algorithm we use for sprinkling causal sets is written in the appendix, and it in principle agrees with the algorithm used in [5]. Basically, we randomly select points in an Alexandrov set and use these points as elements in the causal set; as we already know the number of points we wish to sprinkle before we begin, sprinkling selects a causal set among the ensemble of N-element causal sets and equation (7) is the correct theoretical mean: at least for dimensions 2–5, the $\rho_i = \rho_0$ distribution predicts more chains than are actually found, in particular for higher values of k, while with the effective values for ρ_i the fit is so good that in most cases it is difficult to even see the theory data points, as they lie directly underneath the simulation data points. The effect is less dramatic in higher dimensions, but this is due to the fact that an N-point manifoldlike causal set will have shorter chains if it is embedded in higher dimensions. (We should be able to see the same dramatic differences in higher dimensions if we used enough points for the peak to be in the same place as in the 2D case; however, this is very demanding computationally as the peak is around $N^{1/d}$.)

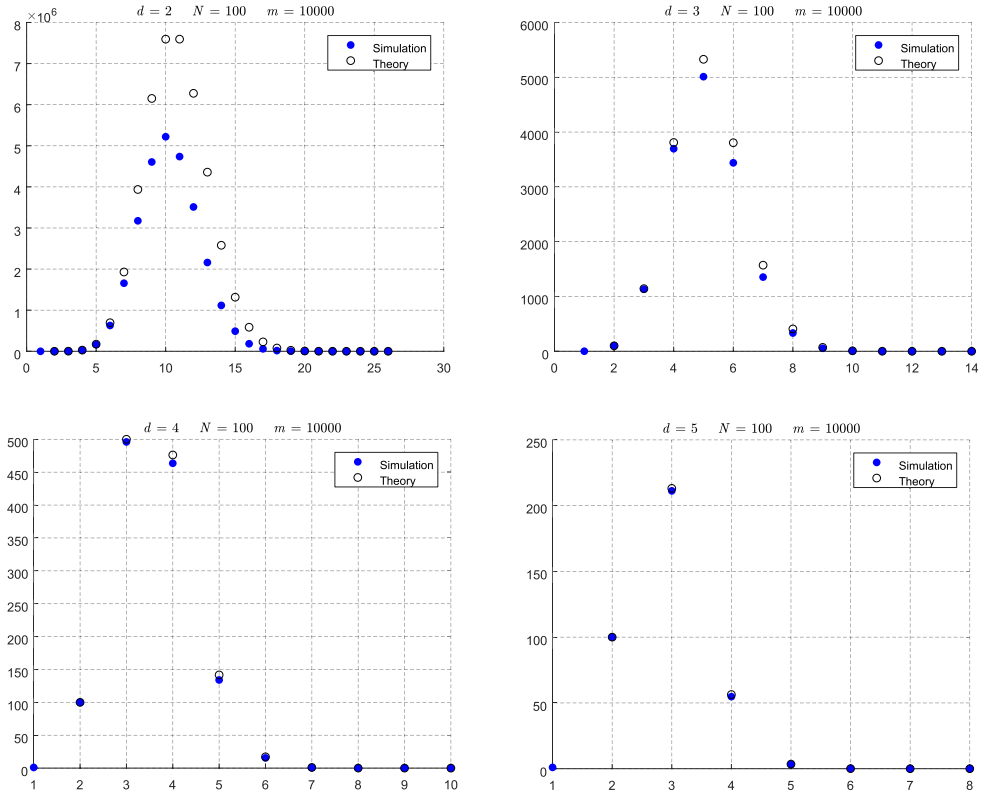

Figure 2. Plots of the average value of c_k as a function of k for $m = 10\,000$ simulated sprinklings of $N = 100$ points in Minkowski space of various dimensionalities, and the mean number $\langle c_k \rangle_0$ of k-chains computed using the fixed density distribution in equation (8).

From the analytical expression for the mean number of chains of length k we can now derive the mean chain length and the width of the chain length distribution. The results of these calculations will be discussed in section 4.

We should note that equation (8) is the correct expression for the average number of chains between the minimal and maximal points of an Alexandrov set of volume V when points are sprinkled inside a much larger d-dimensional flat spacetime with density ρ. In other words, if the number of points in this volume is unknown (but on average $N = \rho V$) the fact that when we place the points along a chain some of the available points have been used to place the previous ones is irrelevant, as infinitely many are available, and the density really is always ρ; however, as we take the view that the manifold is emergent and causal sets are fundamental objects, our formula equation (7) is the one that should be used here. This can be made more obvious by looking at the longest chains; the mean value of $\langle c_k \rangle$ for lengths $k > N + 1$ vanishes identically as no N-element causal set can have chains of such lengths; however, the $\langle c_k \rangle_0$ distribution gives a nonzero mean for all finite lengths as there can be arbitrarily many points in the set.

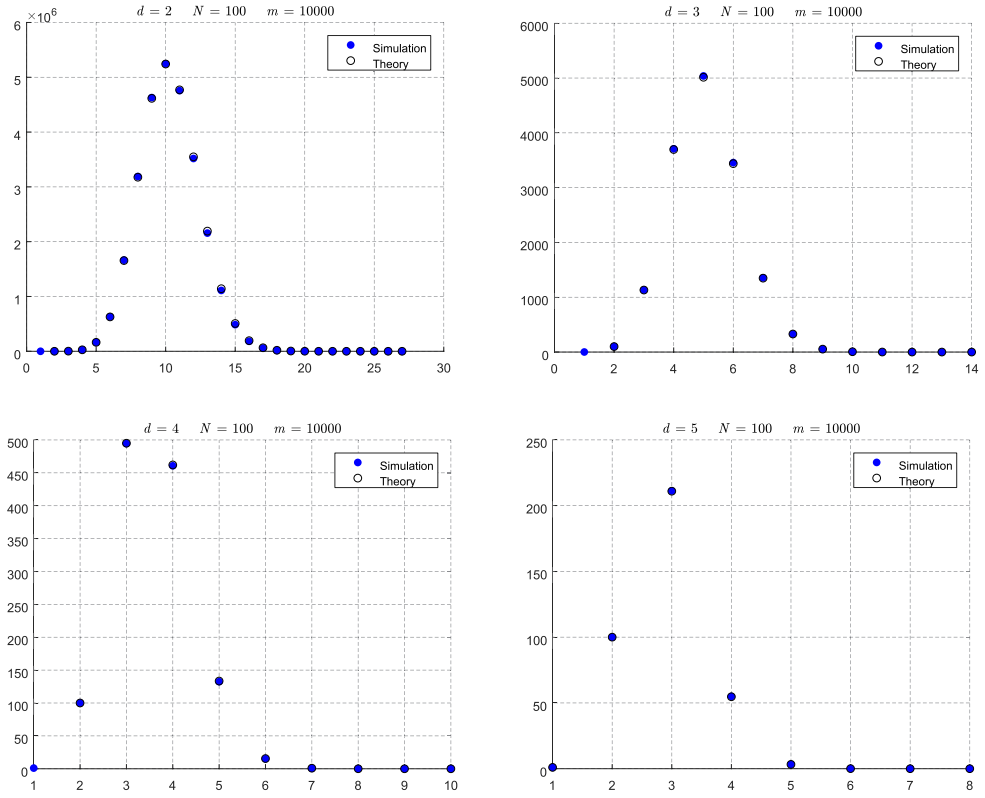

Figure 3. Plots of the average value of c_k as a function of k for $m = 10\,000$ simulated sprinklings of $N = 100$ points in Minkowski space of various dimensionalities, and the mean number $\langle c_k \rangle$ of k-chains computed using the distribution in equation (7) with varying effective densities.

3. Path length distributions in Minkowski space

In this section we derive the path length distribution for a causal set uniformly embedded in Minkowski spacetime. We obtained an expression for this distribution in $d = 2$ dimensions in [2], but here we follow the approach with varying effective densities introduced in the previous section and extend our results to an arbitrary value of d. The setup for the problem is similar to the one used in [2]. We start from an expression for the probability of finding a k-path through a set of locations in Minkowski space analogous to the ones in equations (1)–(3) for the probability of finding a k-chain through that set of locations. The difference is that in the case of paths the probabilities must include factors expressing the requirement that none of the Alexandrov sets $A_{i,i+1}$ contain any other sprinkled points and therefore their union, of volume $V = \sum_i V_{i,i+1}$, be empty,

$$\mathrm{d}P_{(k)}(x_1, ..., x_{k-1}) = (\rho_0\,\mathrm{d}V_1)\,(\rho_1\,\mathrm{d}V_2)\,\cdots\,(\rho_{k-2}\,\mathrm{d}V_{k-1})\left(1 - \frac{\sum_{i=0}^{k-1} V_{i,i+1}}{V_0}\right)^{N-k+1}, \tag{9}$$

for all $2 \leqslant k \leqslant N + 1$ (while now for $k = 1$ the probability vanishes), where the binomial distribution has been used for the probability that the Alexandrov sets are empty, so now the integrated mean number of paths is given by

$$\langle n_k\rangle = \rho_0 \int_{A_0} \mathrm{d}^d x_1\ \rho_1 \int_{A_1} \mathrm{d}^d x_2 \cdots\ \rho_{k-2} \int_{A_{k-2}} \mathrm{d}^d x_{k-1} \left(1 - \frac{\sum_{i=0}^{k-1} V_{i,i+1}}{V_0}\right)^{N-k+1}, \tag{10}$$

where the densities ρ_i were defined in section 2, and the exponent of the argument in the integral is $N-k+1$, as this is the number of remaining points, the ones not in the path. Using a polynomial expansion for the argument we find

$$\begin{aligned}\langle n_k\rangle = {} & \frac{N!}{(N-k+1)!}\frac{1}{V_0^{k-1}} \sum_{i_1=0}^{N-k+1} \binom{N-k+1}{i_1} \left(\frac{-1}{V_0}\right)^{i_1} \sum_{i_2=0}^{i_1} \binom{i_1}{i_2} \\ & \times \cdots \times \sum_{i_k=0}^{i_{k-1}} \binom{i_{k-1}}{i_k} \int_{A_0} \mathrm{d}^d x_1\ V_{0,1}^{i_1-i_2} \int_{A_1} \mathrm{d}^d x_2\ V_{1,2}^{i_2-i_3} \\ & \times \cdots \times \int_{A_{k-2}} \mathrm{d}^d x_{k-1}\ V_{k-2,k-1}^{i_{k-1}-i_k}\ V_{k-1,k}^{i_k}.\end{aligned} \tag{11}$$

These integrals can be explicitly calculated, and the result is

$$\begin{aligned}\langle n_k\rangle = {} & \frac{N!}{(N-k+1)!} \left(\frac{\Gamma(d+1)}{2\Gamma(d/2)}\right)^{k-1} \\ & \times \sum_{i=0}^{N-k+1} \binom{N-k+1}{i} \frac{(-1)^i\,\Gamma(i+1)}{\Gamma((i+k)d/2)\,\Gamma(1+(k-1+i)d/2)} f_{i,k},\end{aligned} \tag{12}$$

where the $f_{i,k}$ are defined by

$$f_{i,1} = \frac{\Gamma((i+1)d/2)\,\Gamma(1+id/2)}{\Gamma(i+1)} \tag{13}$$

for $k = 1$, $0 \leqslant i \leqslant N$, and

$$f_{i,k} = \sum_{j=0}^{i} \frac{\Gamma((i-j+1)d/2)\,\Gamma(1+(i-j)d/2)}{\Gamma(i-j+1)} f_{j,k-1}, \tag{14}$$

for $2 \leqslant k \leqslant N+1$, $0 \leqslant i \leqslant N-k+1$. We will prove the result (12) by induction. Let us assume that the result is correct for $\langle n_k\rangle$, consider the expression for $\langle n_{k+1}\rangle$, and show that we can write the latter in the same form. Written for $\langle n_{k+1}\rangle$, equation (12) becomes

$$\begin{aligned}\langle n_{k+1}\rangle = {} & \frac{N!}{(N-k)!}\frac{1}{V_0^{k}} \sum_{i_1=0}^{N-k} \binom{N-k}{i_1} \left(\frac{-1}{V_0}\right)^{i_1} \sum_{i_2=0}^{i_1} \binom{i_1}{i_2} \cdots \sum_{i_k=0}^{i_k} \binom{i_k}{i_{k+1}} \\ & \times \int_{A_0} \mathrm{d}^d x_1\ V_{0,1}^{i_1-i_2} \int_{A_1} \mathrm{d}^d x_2\ V_{1,2}^{i_2-i_3} \cdots \int_{A_{k-1}} \mathrm{d}^d x_k\ V_{k-1,k}^{i_k-i_{k+1}} V_{k,k+1}^{i_{k+1}}.\end{aligned} \tag{15}$$

We see that this equation has one more integral, resulting in one more parameter and hence one more sum. If we use the result in equation (12), our induction hypothesis, to evaluate the first $k-1$ integrals and the corresponding sums, some simple algebra gives

$$\langle n_{k+1}\rangle = \frac{N!}{(N-k)!}\frac{1}{V_0^k}\left(\frac{\Gamma(d+1)}{2\,\Gamma(\frac{d}{2})}\right)^{k-1}\sum_{i_1=0}^{N-k}\binom{N-k}{i_1}\left(\frac{-1}{V_0}\right)^{i_1}$$
$$\times\sum_{i_2=0}^{i_1}\binom{i_1}{i_2}\frac{\Gamma(i_2+1)}{\Gamma((i_2+k)\frac{d}{2})\,\Gamma(1+(k-1+i_2)\frac{d}{2})}f_{i_2,k}\int_{A_0}\mathrm{d}^d x_1\; V_{0,1}^{i_1-i_2}\,V_{1,k+1}^{i_2+k-1}. \tag{16}$$

The last integral in this expression can be simply calculated using null coordinates defined in terms of the Minkowski time t and radial coordinate $r=(\sum_{i=1}^{d-1}x_i^2)^{1/2}$ as

$$u=(t+r)/\sqrt{2},\qquad v=(t-r)/\sqrt{2}, \tag{17}$$

and one obtains that

$$\int_{A_0}\mathrm{d}^d x_1\; V_{0,1}^{i_1-i_2}\,V_{1,k+1}^{i_2+k-1}$$
$$=V_0^{i_1+k}\,\frac{\Gamma(d+1)}{2\Gamma(\frac{d}{2})}\,\frac{\Gamma(\frac{d}{2}(i_2+k))\,\Gamma(1+\frac{d}{2}(k+i_2-1))}{\Gamma(\frac{d}{2}(i_1+k+1))\,\Gamma(1+\frac{d}{2}(k+i_1))}$$
$$\times\,\Gamma(1+\frac{d}{2}(i_1-i_2))\,\Gamma(\frac{d}{2}(i_1-i_2+1)). \tag{18}$$

After plugging this result back into equation (16) and some simple algebra we obtain

$$\langle n_{k+1}\rangle = \frac{N!}{(N-k)!}\left(\frac{\Gamma(d+1)}{2\,\Gamma(d/2)}\right)^{k}$$
$$\times\sum_{i_1=0}^{N-k}\binom{N-k}{i_1}\frac{\Gamma(i_1+1)}{\Gamma(\frac{d}{2}(i_1+k+1))\,\Gamma(1+\frac{d}{2}(k+i_1))}$$
$$\times\underbrace{\sum_{i_2=0}^{i_1}\frac{\Gamma(\frac{d}{2}(i_1-i_2+1))\,\Gamma(1+\frac{d}{2}(i_1-i_2))}{\Gamma(i_1-i_2+1)}f_{i_2,k}}_{f_{i_1,k+1}}, \tag{19}$$

where we have used the recursion relation defined in equation (14). The above equation is exactly the equation for $\langle n_k\rangle$ with k replaced with $k+1$.

This result is in complete agreement with the 2D case obtained in [2], with the exception of the varying densities mentioned above. It is also interesting to note that the term with $i_1=0$ in the sum corresponds to the number of chains, which was discussed in section 2. We now turn our attention to applications of these distributions.

4. Example: manifoldlikeness

A standing question in causal set theory is how to determine whether a causal set $\mathcal{C}$ is manifoldlike in the sense discussed in section 1. In other words, is there a mapping of the causal set to a manifold $\mathcal{M}$ such that the causal relations are preserved and the points are distributed in a way that faithfully probes the geometry of the continuum? There has been some progress on general aspects of this question, with results showing that if a causal set is manifoldlike, the manifold it reproduces is 'approximately unique' [6, 7]. Our goal here is to address more specific aspects. A study of the manifoldlikeness of specific causal sets was also carried out in [8], based on a different approach.

4.1. Paths

In [2] we argued that a causal set's path length distribution could be used to determine if the set was manifoldlike, at least in Minkowski space, by comparing it to the theoretical one. We will briefly recall this argument here. The path length distributions of manifoldlike causal sets all share a set of characteristics which distinguish them from at least most (perhaps all) non-manifoldlike distributions. Manifoldlike causal sets have strongly peaked, Gaussian-looking path length distributions, as seen from the left part of figure 5, with mean peak position, height and width (and size of fluctuations around those values) depending on d and N in ways that can be obtained from simulations or calculated analytically. Most non-manifoldlike causal sets, however, have path length distributions which are either qualitatively different or do not fit the known dependence on d and N.

While there are many different types of non-manifoldlike causal sets, we will focus on two of the most obvious ones. Most very large causal sets (the fraction goes to 1 as $N \to \infty$) are of the Kleitman–Rothschild type [9]. These causal sets are in three layers, with a fourth of the points being in the top layer, a fourth in the bottom layer, and half in the middle layer; each element in the bottom and top layers is linked to half of the elements in the middle layer, as seen in the example on the left of figure 6. These causal sets are obviously not manifoldlike as their height does not grow with size, and they are thus unable to encode all of the geometric information contained in a manifold, and their path length distribution is proportional to a Kronecker delta at $k = 2$.

The other non-manifoldlike causal sets we will consider are regular lattices. In particular, we will look at 2D and 3D cases in detail because they can be set up differently, but we expect the higher-dimensional cases to give similar results. Regular lattices are probably the most obvious way to discretize a geometry. However, they do not work for Lorentzian geometries in the sense that each one picks a preferred frame and is therefore not Lorentz-invariant. A 2D regular lattice can be set up for example with its lattice sites placed at evenly spaced locations along null lines, as in the right-hand part of figure 6. As the figure shows, each point that is not on the boundary is linked to exactly two other points along 45° lines as measured from the vertical, and all links in this causal set are along one of those lines[2] (also, in this figure the lattice looks square, but that would not be the case in any boosted frame). This means that the path length distribution is again proportional to a Kronecker delta with, in the case of the 11×11 lattice shown, $n_k \propto \delta_{k,20}$.

In the 3D case a regular lattice cannot have all points arranged along null lines, so we consider an example in which they are arranged along t, x and y coordinate lines of a Cartesian coordinate system. An example with again 11 layers in the time direction is shown on the left in figure 7. This lattice has paths of varying lengths, with the longest ones having $k = 10$. The whole path length distribution is shown on the right in figure 7, together with the corresponding average distribution for a sample of 20 causal sets randomly sprinkled in 3D Minkowski space. The two distributions differ in height, peak position and width. While we know that the height of the distributions for random causal sets in Minkowski space can fluctuate considerably, the peak position and width are subject to smaller fluctuations, and can be used to determine that the 3D regular lattice is not manifoldlike.

If we had just seen these distributions, we would be able to determine that they were not manifoldlike. While there are non-manifoldlike causal sets which pass this criterion, at the

[2] Technically, to call these elements linked, we have to either draw the lines to be timelike rather than null, or modify our continuum interpretation of $a \prec b$ to correspond to causal relations as opposed to timelike ones.

very least (for large values of N) this program will allow us to eliminate most non-manifold-like causal sets.

4.2. Chains

We now wish to use a causal set's chain distribution as a measure of manifoldlikeness. This may seem puzzling, as we already have a measure using the path distribution, but the expected number of chains is much easier to calculate, and we have a formula to find the expected number of chains of length k, whereas for paths we only have a recursion relation. Furthermore, it is possible to extend our calculations beyond Minkowski space using Riemann normal coordinates (possibly to an arbitrary order of $RV^{2/d}$ where R is some curvature quantity) allowing us to broaden our measure of manifoldlikeness to causal sets embedded in curved manifolds. From the right of figure 5 we can see that the chain length distribution of causal sets embedded in 2D Minkowski space has a shape similar to that of the path lengths; however, it is much taller, as there are many more chains than paths, and shifted to the left. Let us compare these distributions to those of the Kleitman–Rothschild type and our 2D square lattice. Neither distribution is as simple as its path counterpart. If we add minimal and maximal elements to the Kleitman–Rothschild causal set, our chain length distribution will have one chain of length one, N chains of length two (all chain distributions share these features), and depending on the particular causal set some number of chains of length three and four. It is not quite the Kronecker delta from before, but it is obviously not the Gaussian like distributions of the manifoldlike causal sets. The square lattice, however, is a different story. From figure 8, we can see a number of things: the shape of the square lattice's chain distribution is similar to the theoretical distribution; however, it is much larger. This does not necessarily exclude it from being manifoldlike though, as individual distributions can have huge variations away from the average. What we can do is determine how many standard deviations away from the theoretical average the square lattice is.

Computing $\sigma_k^2 = \langle c_k^2 \rangle - \langle c_k \rangle^2$ is difficult but not impossible; however, the number of terms we have to calculate increases rapidly with k, so let us restrict our attention to the simplest case. In an N-element causal set we always have $c_1 = 1$ and $c_2 = N$, so $k = 3$ gives the first non-trivial mean number of chains. Its standard deviation can be calculated theoretically in the usual way, $\sigma_3^2 = \langle c_3^2 \rangle - \langle c_3 \rangle^2$. We know how to calculate $\langle c_3 \rangle$ and thus $\langle c_3 \rangle^2$, so we're really interested in $\langle c_3^2 \rangle$. Following [4], recall that a chain of length 3 requires an integration over two points, with one to the future of the other; thus, $\langle c_3^2 \rangle$ can be calculated integrating over the positions of four points, or two pairs of points in which one is to the future of the other. There is one caveat: one must proceed cautiously because some of these points can coincide. Let us label the four points i, j, k, ℓ, with $i \prec j$ and $k \prec \ell$, for definiteness. There are six possible cases:

(i) All four points are distinct;
(ii) One coincidence: $i = k$;
(iii) One coincidence: $i = \ell$;
(iv) One coincidence: $j = k$;
(v) One coincidence: $j = \ell$;
(vi) Two coincidences: $i = k, \ell = j$.

We can set up integrals to calculate $\langle c_3^2 \rangle$ for each of these cases; they all proceed trivially (with the exception of the fifth case until one notices that its result should be the same as in

the second case). We should also note that with our density modification, the first case is *not* equivalent to $\langle c_3 \rangle^2$. Putting this together yields

$$\sigma_3^2 = \left(\frac{(N-2)(N-3)}{N(N-1)} - 1 \right) \langle c_3 \rangle^2 + 2 \langle c_4 \rangle + \langle c_3 \rangle + \frac{2N(N-1)(N-2)}{V^3} \int_{A_0} \mathrm{d}^d x_1 \left(\int_{A_1} \mathrm{d}^d x_2 \right)^2, \tag{20}$$

which fits perfectly with simulations. As mentioned above, the others are calculable, but the difficulty increases dramatically with k, and there does not appear to be a general formula. It seems to be a better option to calculate these from simulations; as long as we use a large number of sprinkled causal sets, this should be fine. Results of such simulations are shown in figure 8. At its maximum at $k = 13$, the square lattice's distribution is nearly $15\,\sigma$ away from the theoretical distribution; thus, any reasonable measure of the closeness of these distributions should conclude that the square lattice is *not* manifoldlike. Alternatively, we could have used the peak and width of the distributions to eliminate the square lattice as a manifoldlike causal set. Recall that the chain distributions of manifoldlike causal sets appear to be similar to Gaussians; this means we can characterize them with only two numbers: the peak of the distribution and its width[3]. We can find the peak in the normal way, by differentiating with respect to k and setting the resulting function equal to zero. Doing this yields the following equation which may be numerically solved for $k_{\max}$.

$$\log \frac{\Gamma(d+1)}{2} - \frac{1}{k_{\max}-1} + \psi^0(N - k_{\max} + 2) - \frac{\mathrm{d}\,\psi^0((k_{\max}-1)d/2)}{2} - \frac{\mathrm{d}\,\psi^0(k_{\max} d/2)}{2} = 0, \tag{21}$$

where $\psi^0(x) = \Gamma(x)^{-1}\,\mathrm{d}\Gamma(x)/\mathrm{d}x$. Similarly, we can find the width using this value $k_{\max}$ and numerically solving this equation:

$$\frac{1}{2}\left(\frac{\Gamma(d+2)}{2}\right)^{k_{\max}-2} \frac{1}{\Gamma(N-k_{\max}+2)(k_{\max}-1)\,\Gamma((k_{\max}-1)\frac{d}{2})\,\Gamma(k_{\max}\frac{d}{2})} = \left(\frac{\Gamma(d+2)}{2}\right)^{k-2} \frac{1}{\Gamma(N-k+2)(k-1)\,\Gamma((k-1)\frac{d}{2})\,\Gamma(k\frac{d}{2})}, \tag{22}$$

for which there will be two solutions, k_1 and k_2, with the width being $\Delta := |k_2 - k_1|$. The quantities $(k_{\max}, \Delta)$ should be the average peak and width of chain distributions of causal sets embedded in d-dimensional Minkowski space. If we wanted to use these to develop a secondary criterion for manifoldlikeness, we could proceed as we did above and numerically calculate the variations of each of these quantities; however, these will contain the same information as the σ_k^2's, so we will not do it here.

For comparison, let us consider the chain length distribution for the 3D lattice whose path length distribution was shown in figure 7. In the case of chains, the separation between this distribution and the corresponding ones for random 3D Minkowski causal sets is greater than in the case of paths, but once again we cannot say definitively that this criterion will reject all non-manifoldlike causal sets; however, it will at the very least reject most non-manifoldlike causal sets.

[3] Here we take width to mean full width at half maximum.

5. Example: dimension estimation

In the previous sections we studied the distributions of chain lengths and path lengths for causal sets uniformly embedded in Minkowski spacetime. We also argued that for a general causal set these distributions are detailed enough to provide a lot of information on its embeddability and, if manifoldlike, on the properties of the Lorentzian manifolds in which they can be embedded. As a first application and example of this statement, we consider here how to use these distributions to determine the dimensionality of a flat spacetime manifold in which a manifoldlike causal set is uniformly embedded.

A number of definitions of dimension for posets are available. The ones that are of interest here are ones that when applied to posets obtained from uniform sprinklings of points in d-dimensional Minkowski space give d as the result. The definition of dimension of a poset normally used in combinatorics [10] does not have this property, except when $d = 2$. The available definitions that do have this property are all probabilistic in nature and can be used to determine the effective dimensionality of different regions within a poset at different scales and come in two kinds. In the first kind [4, 11–13], local neighborhoods are identified with intervals $I(p, q)$ within which combinatorial properties of the poset are analyzed, and their volume (cardinality) is used as a measure of the size of each neighborhood. The second kind of definition, that of spectral dimension [14–17], is defined using the heat kernel on the poset, which can be seen as corresponding to a diffusion process in which a particle executes a random walk starting from a given poset element. The scale at which the dimension is determined is set by the number of steps the particle is allowed to take.

Because these definitions are probabilistic, they are subject to possible systematic and statistical errors, in particular for small posets. In some cases the systematic errors can be modeled and corrected for, but in general neither type of error is worrisome if they are used only for posets uniformly embedded in Minkowski space. Our point of view, however, is that if one wants to recover useful information from more general posets, ones that may arise from sprinklings in curved manifolds or non-manifoldlike ones, one should first understand the flat spacetime case. In the more general settings any noninteger values obtained for the dimensionality may well not be due to the same systematic effects or statistical fluctuations, and it becomes important to identify an approach to dimensionality that in Minkowski space is precise even when applied to small regions, and that can possibly be modeled to maximize its accuracy.

In this work we choose to compare the approaches of the first kind above, because with them we do not need to rely on a cutoff as in the spectral dimension approaches and because it appears that the statistical errors are smaller than in approaches of the second kind—though this point deserves to be studied in more detail.

Various methods to estimate the Minkowski dimensionality of posets using intervals to identify local neighborhoods have been proposed. In all of them d is calculated as some function of poset invariants, i.e. quantities that can be defined and calculated (counted) independently of any labeling of its elements; for example, the number of relations, the number of chains of length k, the length $k_{\max}$ of the longest chain, the number of intervals of cardinality n within it, etc—all are quantities which, for a given poset cardinality N, depend on the dimensionality of the space. In the rest of this section we will compare five of those methods and address the following question: Given a poset that is assumed to be embeddable uniformly in an Alexandrov set of Minkowski space, which of these methods would be the most reliable one for estimating its dimensionality?

Our main criterion for comparing the various approaches will be based on precision (rather than accuracy, for reasons that we will explain below) using numerical simulations of posets

in flat space. Specifically, we will generate Minkowski posets by sprinkling N points at random inside an Alexandrov set $A(x,y)$ in d-dimensional Minkowski space; x and y themselves will correspond to p_0 and p_{N+1} in the discrete poset; and the latter will therefore be of the form $\mathcal{C} = \{p_i \mid i = 0, ..., N+1\}$ with $\{p_1, ..., p_N\} = I(p_0, p_{N+1})$.

From a computational point of view one can represent such a poset as one of two types of $(N+2) \times (N+2)$ matrices of 0s and 1s, the matrix of relations $\mathbf{R}$ or the link matrix $\mathbf{L}$, whose elements are defined by

$$R_{ij} = \begin{cases} 1 & \text{if } p_i \prec p_j \\ 0 & \text{otherwise,} \end{cases} \qquad L_{ij} = \begin{cases} 1 & \text{if } p_i \prec\!* \, p_j \\ 0 & \text{otherwise.} \end{cases} \tag{23}$$

The two matrices contain the same amount of information and can be determined from each other:

$$R_{ij} = \begin{cases} 1 & \text{if } \sum_{n=1}^{N} (L^n)_{ij} \geqslant 1 \\ 0 & \text{otherwise} \end{cases} \tag{24}$$

and

$$L_{ij} = \begin{cases} 1 & \text{if } R_{ij} = 1 \text{ and } (R^2)_{ij} = 0 \\ 0 & \text{otherwise.} \end{cases} \tag{25}$$

Notice that the entries in both matrices are always mostly 0s, since $R_{ii} = L_{ii} = 0$ for all i, and $(R_{ij} = 1) \Rightarrow (R_{ji} = 0)$ for all (i,j), with L_{ij} satisfying an analogous property. Notice also that from the powers of $\mathbf{L}$ one can read off the number of paths of any given length, and from the powers of $\mathbf{R}$ one can read off the number of chains of any given length[4]; more precisely, for any $k \geqslant 1$ the number of paths/chains of length k between any two p_i and p_j are

$$n_k(i,j) = (L^k)_{ij}, \qquad c_k(i,j) = (R^k)_{ij}, \tag{26}$$

respectively. In particular, for each poset of this type there exists an integer $l \leqslant N+1$, the height of the poset, such that $\mathbf{R}^l = \mathbf{L}^l \neq \mathbf{0}$ but $\mathbf{R}^{l+1} = \mathbf{L}^{l+1} = \mathbf{0}$ as matrices.

5.1. Midpoint approach

The midpoint dimension of a poset [11] is obtained as follows. Choose a point p_m in $\mathcal{C}$ such that the cardinality n of the smaller of the two resultant intervals $I_\downarrow = I(p, p_m)$ and $I_\uparrow = I(p_m, q)$ is as large as possible. (Alternatively, we could choose a point such that the larger of the resulting intervals is as small as possible; simulations we performed show that in that case, or if we used a symmetric combination of the two, the results would be equivalent.) If the overall N is large enough, then this point is most likely in the middle of the big interval, in the sense that the two smaller intervals will have approximately equal volumes and they will be the largest ones for which this is the case. If $\mathcal{C}$ was uniformly embedded in a flat continuum spacetime, the height of each of $I_\downarrow$ and $I_\uparrow$ would then be approximately half of that of $\mathcal{C}$ and, because their volumes scale as the dth power of their height,

$$v = \frac{V}{2^d}, \tag{27}$$

where V is the volume of $I(p,q)$, and v the volume of the smaller of $I_\downarrow$ and $I_\uparrow$ in the continuum. But in a poset obtained from a uniform sprinkling of points in a manifold the number N

[4] This only works if the irreflexive version of the partial order is used.

of elements in each region is proportional to its volume, so we expect to find $N/n = V/v = 2^d$, and the Minkowski dimension of the set can estimated as

$$d = \frac{\ln(N/n)}{\ln(2)}. \tag{28}$$

Figure 10 shows the estimated dimension, calculated in this approach using equation (28), for values of N in the range $100 \leqslant N \leqslant 1500$ in $d = 2$, 3, 4 and 5 dimensions. For each value of d and N, 20 different Minkowski posets were obtained from random point sprinklings in flat spacetime; the error bars show the standard deviations for the 20 corresponding d estimates. What the figure shows is that, in addition to statistical fluctuations that decrease in size for large N and grow for large d, the use of equation (28) introduces a systematic error that also decreases with N and increases with d. At least part of this error is due to the fact that because of how it is defined, v is in general smaller than the value given by equation (27).

5.2. Modified Myrheim-Meyer approach

In [4] Meyer proposed a way to estimate the Minkowski dimension of a poset, known as the Myrheim-Meyer dimension, using the expected number of chains in an Alexandrov set of Minkowski space based on a Poisson point sprikling; to use it, one calculates the number c_3 of three-chains in a given causal set and inserts this into equation (8) with $k = 3$ for the expected number of three-chains. This gives

$$\frac{c_3}{N^2} = \frac{1}{4}\frac{\Gamma(d+1)\,\Gamma(d/2)}{\Gamma(3d/2)}, \tag{29}$$

which can be solved numerically for d. In our context, since we compare the causal set of interest with others of the same cardinality N embedded in Minkowski space, our modified equation (7) provides a better estimate for the expected number of chains; however, because only chains of length 3 are used and the effect of our density variation is smaller for chains of smaller length, this modified Myrheim-Meyer dimension deviates only slightly from the original, particularly for large causal sets. Using our equation,

$$\frac{c_3}{N(N-1)} = \frac{1}{4}\frac{\Gamma(d+1)\,\Gamma(d/2)}{\Gamma(3d/2)}. \tag{30}$$

Figure 11 shows the estimated dimension, calculated using equation (30), for values of N in the range $100 \leqslant N \leqslant 1500$ in $d = 2$, 3, 4 and 5 dimensions. For each value of d and N, 20 different Minkowski posets were obtained from random point sprinklings in flat spacetime; the error bars show the standard deviations for the 20 corresponding d estimates. Because this estimate relies on the exact relation (30), rather than on an approximate relationship between discrete and continuum quantities, the figure only shows statistical fluctuations, that again decrease in size for large N and grow with d.

5.3. Brightwell–Gregory approach

The Brightwell–Gregory method [12] for calculating the dimension of a Minkowski poset is based on the length of the longest path in the poset. If an N-element poset is uniformly sprinkled inside an Alexandrov set of volume V in Minkowski space, the longest path (longest chain) in it can be thought of as a discretized geodesic between the maximal and minimal points. Its length $k_{\max}$ should then be approximately proportional to the proper time from p_0

to p_{N+1}, which in the continuum is in turn proportional (with a known proportionality coefficient) to $V^{1/d}$. This leads to defining a coefficient $\beta_{d,N}$ by

$$k_{\max} = \beta_{d,N} N^{1/d}. \tag{31}$$

From simulations it appears that $\beta_{d,N}$ is only weakly dependent on N and in the large-N limit, when endpoint effects become unimportant, it is expected to approach a well-defined value

$$\beta_d := \lim_{N\to\infty} \beta_{d,N}. \tag{32}$$

Brightwell and Gregory found [12] that in two dimensions $\beta_2 = 2$, and for arbitrary dimensionality $d \geqslant 3$ we have

$$1.77 \leqslant \frac{2^{1-1/d}}{\Gamma(1+1/d)} \leqslant \beta_d \leqslant \frac{2^{1-1/d}\,\mathrm{e}\,\Gamma(d+1)^{1/d}}{d} \leqslant 2.62. \tag{33}$$

These upper and lower bounds on β_d are plotted as functions of d in figure 12. We can both infer from such plots and find analytically that $\beta_d \to 2$ as $d \to \infty$, and these results are consistent with $\beta_d = 2$ for all d, but we are not aware of results to this effect. It is interesting to note that, while these bounds allow a greater range of values for β_d above 2 than below 2, it appears from the results of our simulations, shown in figure 12, that for low values of N all $\beta_{d,N}$ are below 2. Those results were obtained generating, for each d between 2 and 5 and values of N between 100 and 1500, 15 random Minkowski posets, finding the length $k_{\max}$ of the longest chain in each of them, and averaging the 15 estimated values of $\beta_{d,N}$ obtained from equation (31).

In this approach, the Minkowski dimension of a given poset can be estimated by finding $k_{\max}$ and solving for d the defining relation for $\beta_{d,N}$, that can be written as

$$d = \frac{\ln(N)}{\ln(k_{\max}/\beta_{d,N})}. \tag{34}$$

The most accurate estimate for d would be obtained if we had a theoretical value for $\beta_{d,N}$ available for the given N and for all d in some range, and found a d that solves equation (34) exactly, possibly using numerical methods. In the absence of such an exact expression we could produce approximate values of d centered around the correct ones using for $\beta_{d,N}$ the average of the values obtained from some set of simulations, for example the ones shown in figure 12, for each pair of values of (d,N). This would improve the accuracy of the estimates for d but leave their precision essentially unaffected, so we chose not to do it and use $\beta = 2$ in all estimates, which explains the offset of the results shown in figure 13, obtained with the same set of values for (d,N).

5.4. Average path length approach

The approach we proposed in [2] to estimating the Minkowski dimension of a poset is based on the distribution of path lengths in it. Examples of such distributions were shown in figure 4 for posets obtained from Minkowski space sprinklings. In these examples the curves are bell-shaped, with an average length $\bar{k}$ and full width at half maximum Δ that differ for different values of d; if the number of points is kept constant, as the dimension increases both $\bar{k}$ and Δ tend to smaller values because of the extra volume introduced by the extra dimensions; the shape of the distribution however remains the same for all dimensions. When estimating d, this encourages us to use the average path length $\bar{k}$, as a quantity that may be subject to smaller statistical fluctuations than $k_{\max}$.

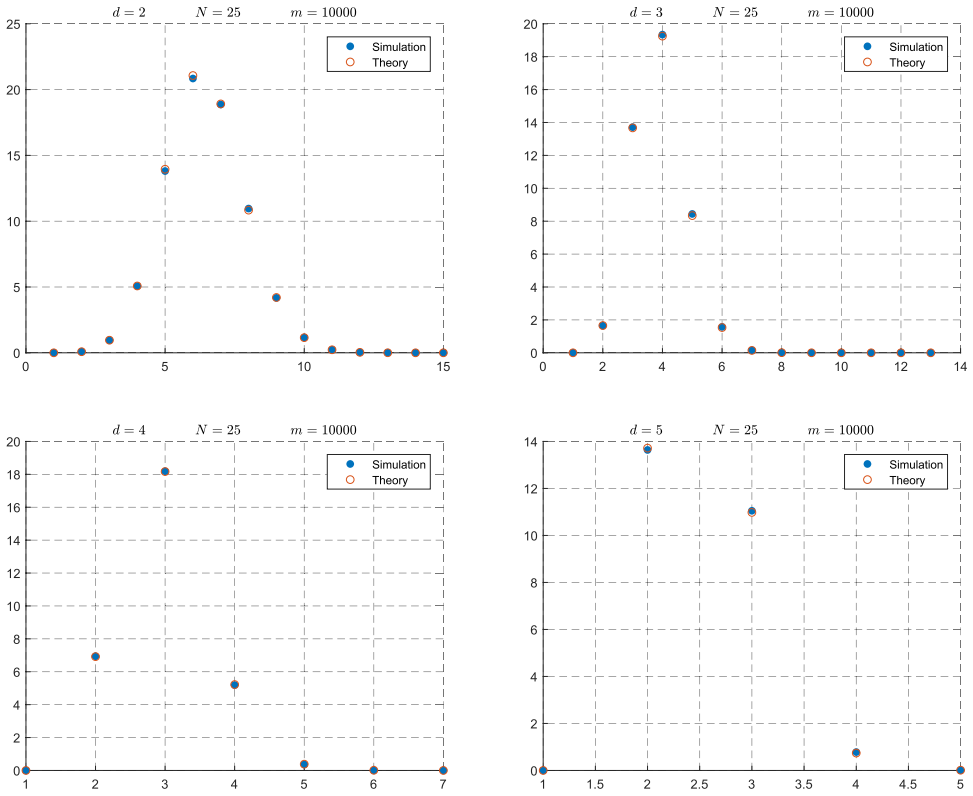

Figure 4. Plots of the average value of n_k as a function of k for $m = 10\,000$ simulated sprinklings of $N = 25$ points in Minkowski space of various dimensionalities, and the mean number $\langle n_k \rangle$ of k-paths computed from the path length distribution (12) that uses the varying effective densities.

The average path length in a poset sprinkled in Minkowski space can be numerically calculated as follows. We first find the total number of k-paths n_k and the total number of paths N_{paths} between the minimal and maximal elements using the link matrix,

$$n_k = (L^k)_{0,N+1}, \qquad N_{\text{paths}} = \sum_{k=1}^{N+1} n_k. \tag{35}$$

Notice that $N + 1$ is the longest possible path length (in fact, $k = N + 1$ is only achieved when the poset is totally ordered), but in practice in a simulation the summation for N_{paths} can be stopped after $k = l$ if it is found that $(L^l)_{ij} = 0$ for all (i, j). Using these quantities, the average path length can then be found simply as

$$\bar{k} = \frac{1}{N_{\text{paths}}} \sum_{k=1}^{N+1} k\, n_k. \tag{36}$$

As for k_{max} in the Brightwell–Gregory approach, in the large-N limit the average path length in any given number of dimensions will be proportional to $N^{1/d}$, so we can write down an analogous relation between $\bar{k}$ and N, of the form

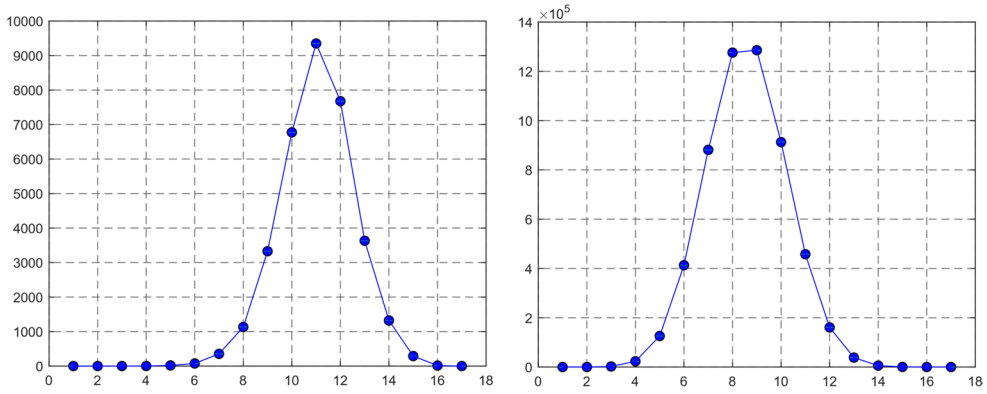

Figure 5. Plots of the path and chain length distributions n_k and c_k (left and right, respectively) as functions of k, for a single causal set of size $N = 100$ embedded in 2D Minkowski space.

$$\bar{k} = \alpha_{d,N} N^{1/d}. \tag{37}$$

An interesting aspect of our approach is that it is in fact possible in principle to numerically calculate exact values for $\alpha_{d,N}$ [2]. We could then rewrite equation (37) as

$$d = \frac{\ln(N)}{\ln(\bar{k}/\alpha_{d,N})}, \tag{38}$$

and, using the theoretically derived values of $\alpha_{d,N}$, find the d that solves equation (38) exactly, at least in principle and again possibly using numerical methods. The problem is that the size of the numbers used to calculate those exact values is a fast growing function of N, so we will rely on values of α derived from simulations instead. Figure 14 shows the approximate values estimated using 500 Minkowski space sprinklings in $d = 2$, 3, 4, 5 and various values of N up to 1500. The error bars shown indicate the standard deviation of the results obtained from the 500 sprinklings generated for each d and N, and are due to statistical fluctuations in the value of the average $\bar{k}$. (For reference, the computing time for each 1000-point sprinkling with $d = 2$, for example, on a regular laptop computer with a 2.3 Gz Intel Core i5 processor is less than a minute, a number that can be better appreciated if we consider that the total number of paths in the resulting poset is $N_{\text{paths}} \approx 3 \times 10^{16}$.)

An interesting observation is that, based on figure 14, $\alpha_{d,N}$ appears to be only weakly dimension dependent, and for each d it appears to tend to an asymptotic value between 1.10 and 1.15 for large values of N. The dimension estimates for the posets generated with the above values for d and N are shown in figure 15 where, for reasons similar to the ones explained in section 5.3 in connection with the Brightwell–Gregory approach, the value of α we used in equation (38) to estimate d was 1.15 for all (d, N).

5.5. Interval size approach

Finally, it is worth mentioning another article [8] in which the authors calculate the characteristic shape of the distribution of interval sizes, as a tool for defining local and non-local neighborhoods. The distribution has the form

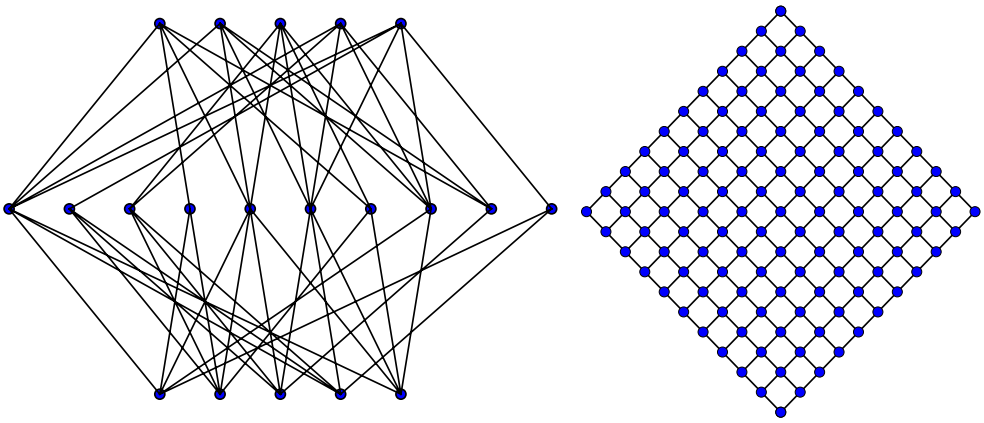

Figure 6. Left: a Kleitman–Rothschild causal set. Right: an 11×11 square lattice.

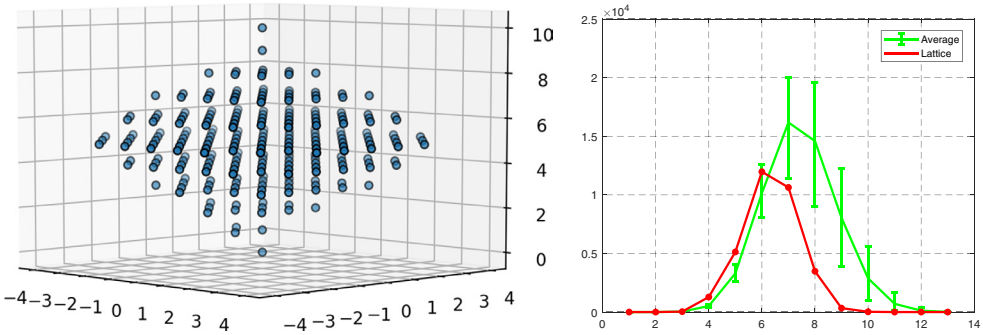

Figure 7. Left: a 3D 'square' lattice (actually a cubic lattice in spacetime); the figure shows the portion of the lattice inside the Alexandrov set of the minimal and maximal points, which has $N = 235$ points. Right: path length distributions for this square lattice and for the average over 500 random sprinklings of 235 points in 3D Minkowski space; the error bars indicate the range of values corresponding to the 50th percentile above and below the average.

$$\langle a_k \rangle = \frac{\Gamma(d)^2}{k!}(-N)^{k+2}\sum_{n=0}^{\infty}\frac{(-N)^n}{n!}\frac{1}{(n+k+1)(n+k+2)} \tag{39}$$

$$\begin{aligned}&\times \frac{\Gamma\left(\frac{d}{2}(n+k)+1\right)}{\Gamma\left(\frac{d}{2}(n+k+2)\right)}\frac{\Gamma\left(\frac{d}{2}(n+k+1)+1\right)}{\Gamma\left(\frac{d}{2}(n+k+3)\right)}\\ =&\frac{N^{k+2}}{(k+2)!}\Gamma(d)^2\frac{\Gamma\left(\frac{d}{2}(k+1)+1\right)\Gamma\left(\frac{d}{2}k+1\right)}{\Gamma\left(\frac{d}{2}(k+1)+d\right)\Gamma\left(\frac{d}{2}k+d\right)}\\ &\times {}_dF_d\left(\begin{matrix}k+1,\frac{2}{d}+k,\cdots,\frac{2(d-1)}{d}+k\\ 3+k,\frac{2}{d}+k+2,\cdots,\frac{2(d-1)}{d}+k+2\end{matrix}\middle|-N\right).\end{aligned} \tag{40}$$

As the authors point out in [8], for each k the values obtained from this expression for different d are well separated, and $\langle a_k \rangle$ is a promising quantity to look at as a dimension estimator. In order to compare it with the other methods we have described, we would need to

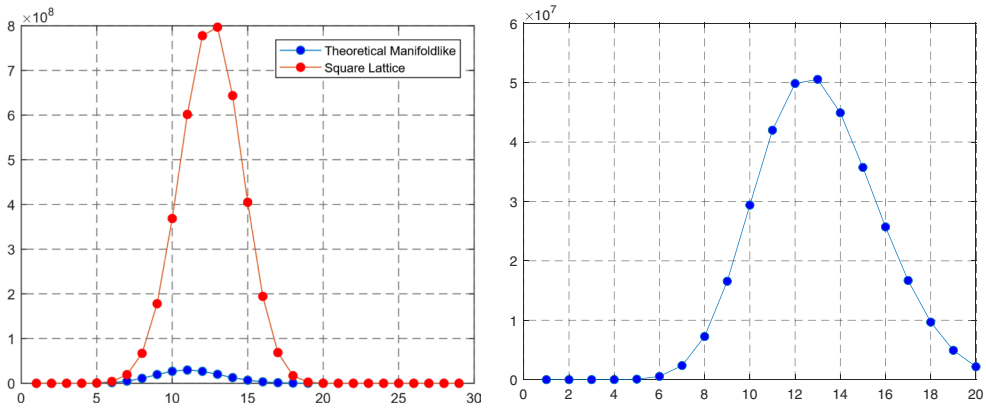

Figure 8. Left: plot of the chain distributions of the 2D 11×11 square lattice and the theoretical average chain distribution for causal sets of size $N = 119$ embedded in 2D Minkowski space; Right: plot of the standard deviation of each c_k for the 119-point 2D Minkowski causal sets on the left, as a function of k.

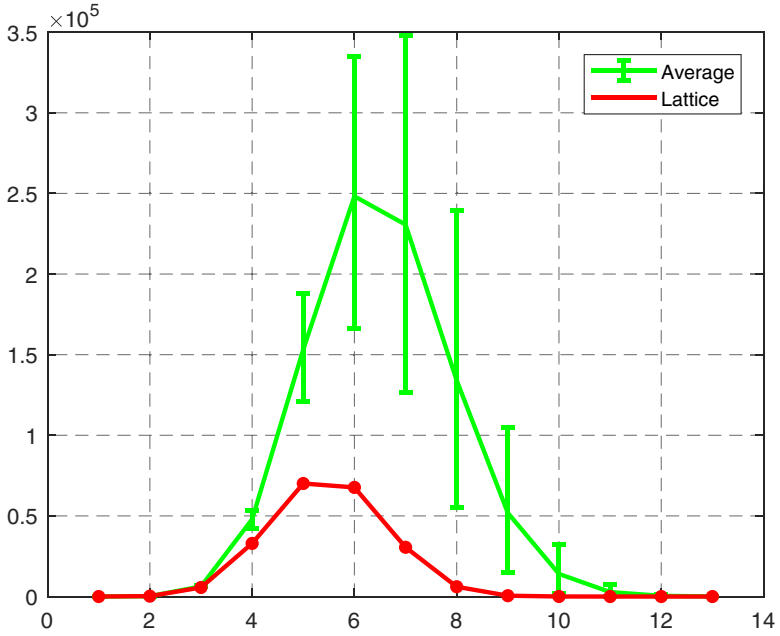

Figure 9. Comparison between the chain length distribution for the 3D square lattice and the average of the chain length distributions for the causal sets obtained from 500 random sprinklings of 235 points in 3D Minkowski space; the error bars indicate the range of values corresponding to the 50th percentile above and below the average.

estimate d for a number of sprinkled causal sets in Minkowski space and calculate the average and standard deviation of those estimates for each k and manifold dimensionality. But in this respect the expressions in (39) and (40) are different from the ones that other dimension estimators are based on. With some of the latter an estimate of d can be obtained for each causal set from explicit expressions, as in (28), (34) and (38); in the method based on three-chains we

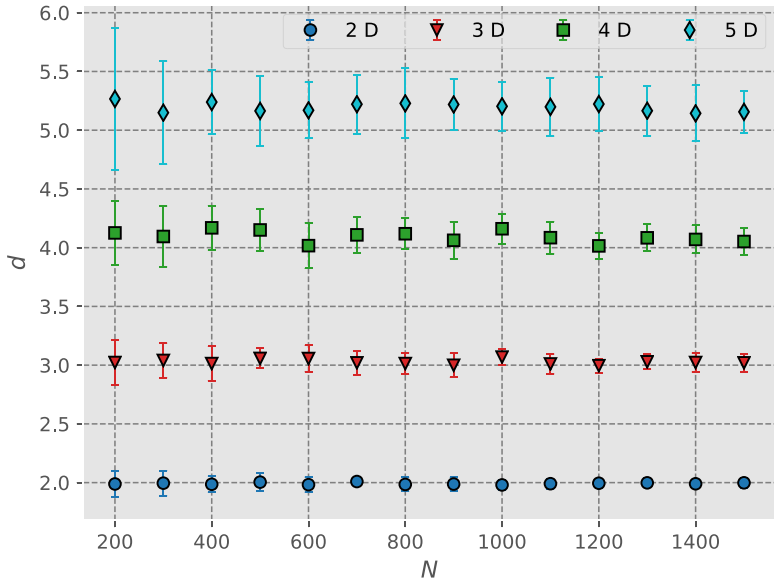

Figure 10. The estimated dimension of Minkowski space calculated using the midpoint approach from simulations in $d = 2$, 3, 4 and 5 dimensions as a function of N. The error bars indicate the standard deviation of the results obtained from 20 sprinklings generated for each d and N.

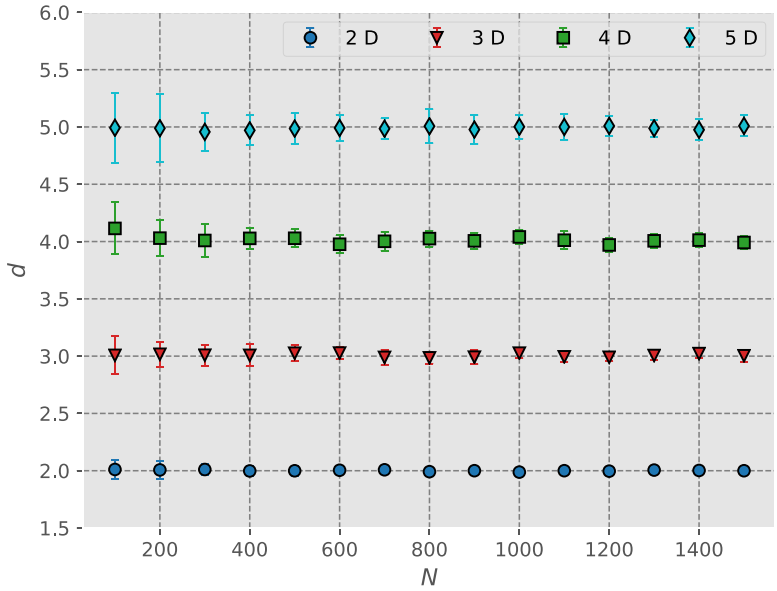

Figure 11. The estimated dimension of Minkowski space calculated using the modified Myrheim-Meyer approach from simulations $d = 2$, 3, 4 and 5 dimensions as a function of N. The error bars indicate the standard deviation of the results obtained from 20 sprinklings generated for each d and N.

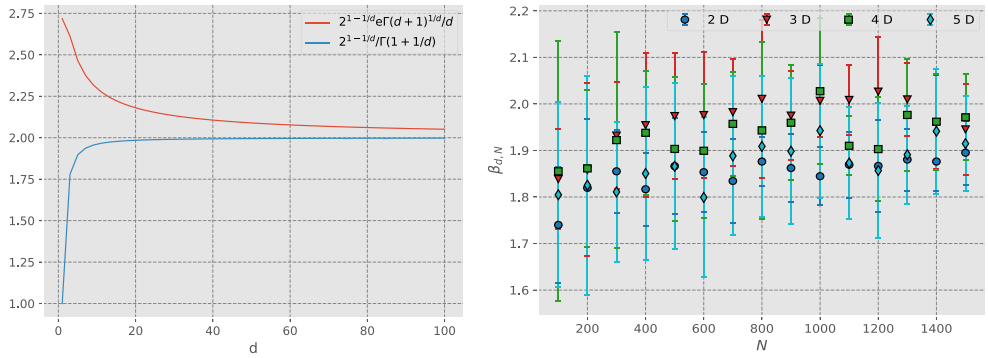

Figure 12. Left: upper and lower bounds on the Brightwell–Gregory parameter β_d as functions of d. Right: the value of $\beta_{d,N}$ for various dimensionalities as a function of N. The error bars indicate the standard deviation of the results obtained from 15 sprinklings for each d and N.

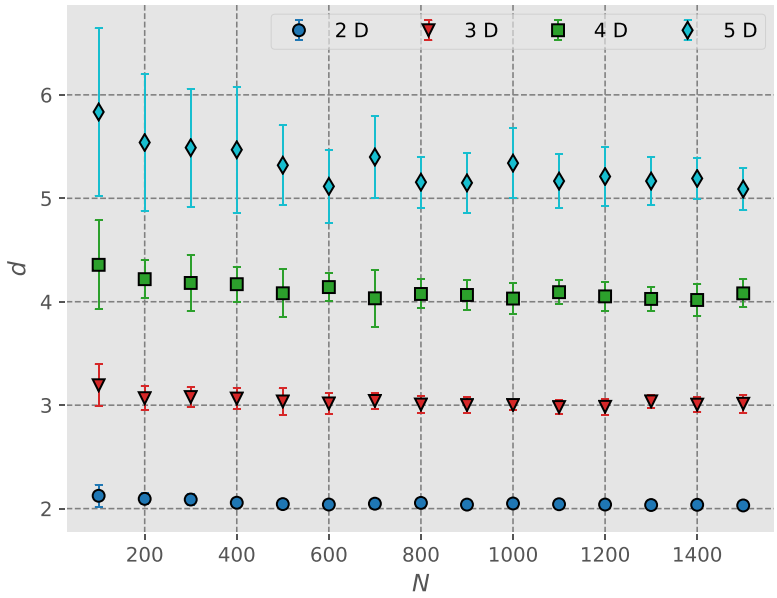

Figure 13. The estimated dimension of Minkowski space in the Brightwell–Gregory approach from simulations in $d = 2, 3, 4$ and 5 dimensions as a function of N. The error bars indicate the standard deviation of the results obtained from 20 sprinklings for each value of d and N.

did not solve equation (30) explicitly for d, but we were still able to find numerically the value of d that solved that equation for each given value of c_3. In the present case, however, equations (39) and (40) cannot be solved explicitly for d, and in trying to solve them numerically we run into the difficulty that (39) involves an infinite sum, and the right-hand side of (40) is only defined for integer values of d.

We can still get an idea of the potential usefulness of this method from an asymptotic formula obtained by the authors [8] for the ratio of the number of intervals of size k to that of intervals of size 0. In the $N \to \infty$ limit (or $\rho \to \infty$ with V_0 fixed) the ratio only depends on the dimension,

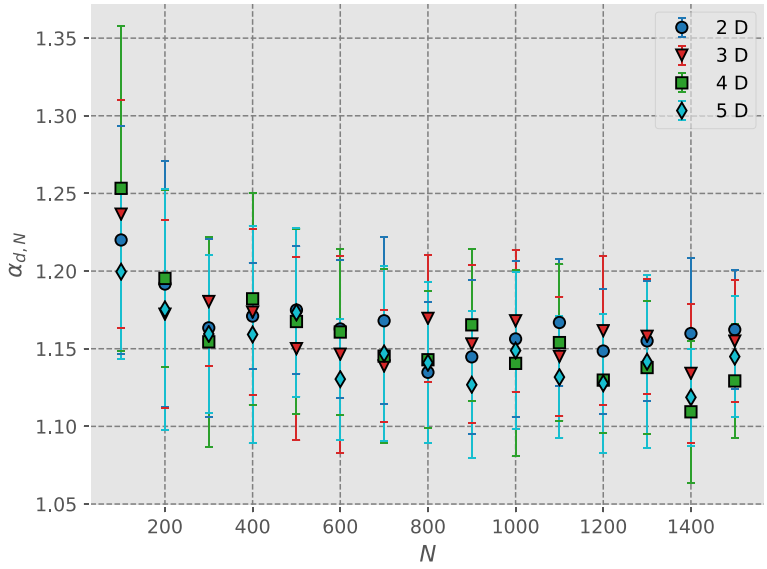

Figure 14. The value of $\alpha_{d,N}$ for various dimensionalities as a function of N. The data point for each $\alpha_{d,N}$ is the average of the values calculated using equation (37) for 15 sprinklings, and the error bars indicate the standard deviation of those 15 values.

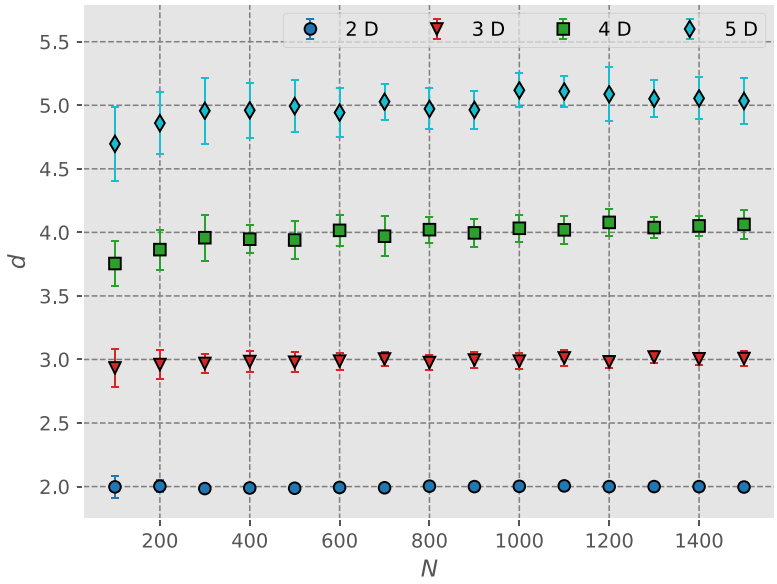

Figure 15. The estimated dimension of Minkowski space calculated using the average path length approach as a function of N, from simulations in $d = 2$, 3, 4 and 5 dimensions. The error bars indicate the standard deviation of the results obtained from 20 sprinklings generated for each d and N.

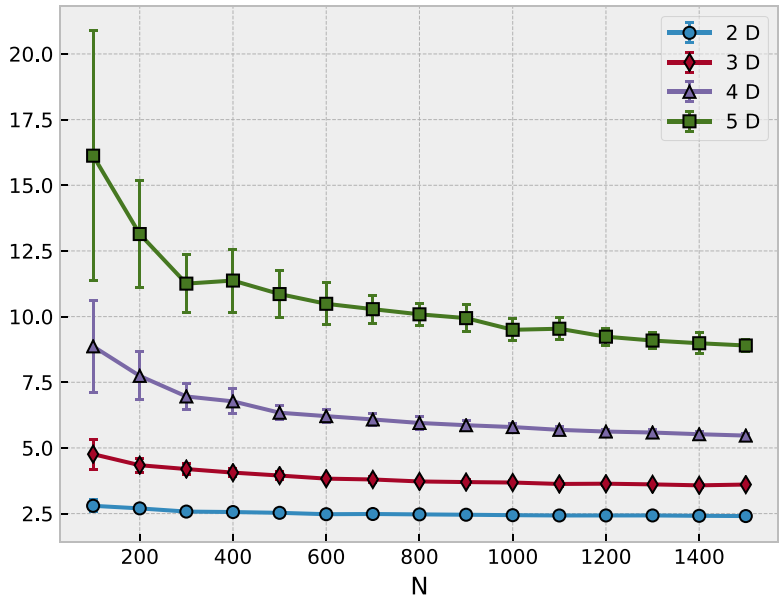

Figure 16. The estimated dimension of Minkowski space calculated using the interval size approach as a function of N with $k = 1$, from simulations in $d = 2$, 3, 4 and 5 dimensions. The error bars indicate the standard deviation of the results obtained from 20 sprinklings generated for each d and N.

$$\lim_{N\to\infty} \frac{\langle a_k \rangle}{\langle a_0 \rangle} = \frac{\Gamma(2/d + k)}{\Gamma(2/d)\,\Gamma(k+1)}. \tag{41}$$

Using this formula with values of a_1 and a_0 from causal sets sprinkled in Minkowski space to estimate d gives the results shown in figure 16. The value obtained for d is not a good estimate for the dimension because the asymptotic formula (41) is being used with relatively small values of N, but the size of the error bars does indicate that the precision of this method might compare favorably with that of the other approaches.

6. Conclusions

The purpose of this paper was to calculate the expected distributions of chain and path lengths for causal sets embeddable in d-dimensional Minkowski space, and point out the two different notions of this concept. One could be referring to either the average of the ensemble of all causal sets embeddedable in an Alexandrov set of fixed volume that on average has density ρ or the average of the ensemble of all N-element causal sets. We argued the latter was more natural and showed that the calculations are inequivalent: the second case involves using a modified effective density. The effects of this variation in the density on the length probability distributions are not negligible, but they can be treated relatively easily. We then showed that these calculations can be used in a comparison between a particular causal set's chain/path length distribution with the expected distribution for a Minkowski-like causal set to determine if the causal set is embeddable in Minkowski space (or, if not, how close it is to being embeddable), and if it is to determine its dimension. Compared to paths, chain lengths have the

benefit that their distribution as a whole is known explicitly, and this analytical result makes it simpler to use in different situations.

We also discussed different types of non-manifoldlike causal sets that are dominant in numbers, the Kleitman–Rothschild type causal sets, and the frequently used ones based on regular lattices, and showed that our criterion is precise enough to eliminate them as manifoldlike. While it appears that most non-manifoldlike causal sets are disqualified by this criterion, nonetheless, one can use the whole distribution or the reduced parameter space (peak position, full width at half maximum, and the total number of paths) to define a manifoldlikeness measure for general causal sets. This is important in particular if we are to consider causal sets with some roughness at microscopic scales.

The above results can be applied to manifoldlike causal sets to obtain their dimension. Even in these general terms, this question is of interest, but it had already been addressed by various satisfactory approaches to dimension estimation, including ones based on exact theoretical calculations. Of the approaches we looked at in our comparison of the results obtained for numerically simulated, uniformly distributed posets in Minkowski space, the best one in terms of the size of the statistical fluctuations for all values of N is the modified Myrheim-Meyer method, based on the number of relations $\langle c_3 \rangle$. One reason why we were interested in the size of the relative fluctuations in the dimension estimates for small posets is that we view the study of Minkowski posets as a first step in the study of more general manifoldlike posets, and we expect small subsets of posets embeddable in curved Lorentzian geometries to be close enough to Minkowski posets that they can be used to obtain dimensional information. Our method, based on the average path length $\bar{k}$, was not quite as good as the modified Myrheim-Meyer method when estimating the dimension of posets known to be embeddable in Minkowski space, but it is based on the whole distribution of path lengths, which contains additional useful information.

Since the dimensionality of a manifold is an integer number and all or most of the methods described here (with the possible exception of the Brightwell–Gregory approach) show relatively small fluctuations, if all posets we consider were known to be manifoldlike there would be various approaches we could use. However, the vast majority of posets are not manifoldlike ([2] discusses this point in a little more detail), so we would in fact like to be able to extend our method to some of the non-manifoldlike ones and obtain from it information on the type of obstruction to their embeddability, at least when they are close to being manifoldlike in an appropriate sense. In the latter case, an estimate of d might give a value that is close to, but does not coincide with one corresponding to an integer dimension. This is the reason why both small statistical fluctuations and accurate theoretical modeling are important.

Appendix

In this appendix we will detail an algorithm for finding the chain (path) length distribution in a causal set. When written in a computer language, the algorithm will be about 20–30 lines long, depending on the language. Several parts could be optimized, but this would not significantly alter the speed as the vast majority of the time the algorithm is running, it is performing matrix multiplication.

(i) Sprinkle points: consider an Alexandrov set in d-dimensional Minkowski space and sprinkle N uniformly random points in it. As a result the entire set will have $N + 2$ elements, including the minimal element, labelled element 0, and the maximal element, labelled element $N + 1$. Without loss of generality, we can assume that the minimal and maximal elements are along the time axis and the values of their spatial

coordinates are all zero. In this coordinate system the coordinates of all elements can be described by a single $d \times (N+2)$ matrix x_{ij}, where this entry in the matrix is the value of the ith coordinate of the jth element. The minimal point then has coordinates $x_{0,0} = -\tau/2,\ x_{1,0} = x_{2,0} = \cdots = x_{d-1,0} = 0$, and the maximal point has coordinates $x_{0,N+1} = \tau/2,\ x_{1,N+1} = x_{2,N+1} = \cdots = x_{d-1,N+1} = 0$. Note that the Alexandrov set has height τ. Now, we must determine the coordinates of the N elements between the maximal and minimal elements. To do this, we will randomly select points in a d-dimensional cube with side lengths τ which has the Alexandrov set centered inside of it. If the points are inside the Alexandrov set (i.e. if they are timelike related to the maximal and minimal points), we accept these points and use them as coordinates of one of the elements; otherwise, we reject them[5].

$i = 1$
  while $i \leqslant N$
    for $j = 0 : d-1$
      $H_j = \text{rand}(-\tau/2, \tau/2)$
      if $\left((x_{0,0} - H_0)^2 > \sum_{m=1}^{d-1} H_m^2 \text{ and } (x_{N+1,0} - H_0)^2 > \sum_{m=1}^{d-1} H_m^2\right)$
        for $k = 0 : d-1$
          $x_{ki} = H_k$
        end for
        $i = i + 1$
      end if
    end for
end while

(ii) Find the relations matrix: once the coordinates of the manifold points the causal set elements are mapped to have been determined, finding the relations matrix is simple. Recall

$$R_{ij} = \begin{cases} 1 & \text{if } p_i \prec p_j \\ 0 & \text{otherwise,} \end{cases} \tag{A.1}$$

so $R_{i,j}$ is only nonzero if the ith element is to the chronological past of the jth one,

$R_{ij} = 0 \ \ \forall i, j$
for $i = 0 : N+1$
  for $j = 0 : n+1$
    if $\left(x_{0,i} < x_{0,j} \text{ and } (x_{0,i} - x_{0,j})^2 > \sum_{k=1}^{d-1} (x_{k,i} - x_{k,j})^2\right)$
      $R_{ij} = 1$
    end if
  end for
end for

[5] This is not the most efficient way to sprinkle. We could have instead defined some function to allow us to select a time coordinate randomly taking into account the fact that there is less volume as one travels away from the center of the Alexandrov set; however, for values of N in the thousands or possibly even more, it wastes very little time to sprinkle into a cube with our acceptance/rejection scheme.

(iii) Find the chain length distribution: we want to find the number of chains of various lengths between the minimal and maximal elements. In general the number of chains of length k between the ith and jth point is

$$c_k(i,j) = (R^k)_{ij}. \tag{A.2}$$

What we want then is $c_k(0,n+1)$ for all values of k. Also, there exists some integer $l \leqslant N+1$ such that $\mathbf{R}^l \neq \mathbf{0}$ but $\mathbf{R}^{l+1} = \mathbf{0}$.

$\mathbf{A} = \mathbf{R}$
$k = 1$
while $\mathbf{A} \neq \mathbf{0}$
  $c_k = A_{0,N+1}$
  $k = k + 1$
  $\mathbf{A} = \mathbf{A} * \mathbf{R}$
end while

This code will find a vector c with l entries such that c_i is the number of chains of length i between the minimal and maximal elements. It can be slightly modified to provide the number of paths rather than chains by defining L_{ij}:

$$L_{ij} = \begin{cases} 1 & \text{if } R_{ij} = 1 \text{ and } (R^2)_{ij} = 0 \\ 0 & \text{otherwise,} \end{cases} \tag{A.3}$$

and using $\mathbf{L}$ instead of $\mathbf{R}$ in the last section of code.

ORCID iDs

L Bombelli https://orcid.org/0000-0002-3471-359X
B B Pilgrim https://orcid.org/0000-0002-2993-8591

References

[1] Bombelli L, Lee J, Meyer D and Sorkin R D 1987 Space-time as a causal set *Phys. Rev. Lett.* **59** 521–4
[2] Aghili M, Bombelli L and Pilgrim B B 2018 Path length distribution in two-dimensional causal sets *Eur. Phys. J.* C **78** 744
[3] Bombelli L, Henson J and Sorkin R D 2009 Discreteness without symmetry breaking: a theorem *Mod. Phys. Lett.* A **24** 2579–87
[4] Meyer D 1988 The dimension of causal sets *PhD Thesis* (Cambridge, MA: MIT)
[5] Cunningham W and Krioukov D 2018 Causal set generator and action computer *Comput. Phys. Commun.* **233** 123
[6] Bombelli L, Tafoya J and Noldus J unpublished
[7] Bombelli L 2000 Statistical Lorentzian geometry and the closeness of Lorentzian manifolds *J. Math. Phys.* **41** 6944–58
[8] Glaser L and Surya S 2013 Towards a definition of locality in a manifoldlike causal set *Phys. Rev.* D **88** 124026
[9] Kleitman D and Rothschild B 1975 Asymptotic enumeration of partial orders on a finite set *Trans. Am. Math. Soc.* **205** 205–20
[10] Kelly D and Trotter W T 1982 Dimension theory for ordered sets *Ordered Sets* ed I Rival (Reidel)
[11] Bombelli L 1987 Space-time as a causal set *PhD Thesis* (Syracuse, NY: Syracuse University)
[12] Brightwell G and Gregory R 1991 Structure of random discrete spacetime *Phys. Rev. Lett.* **66** 260–3

[13] Reid D D 2003 Manifold dimension of a causal set: tests in conformally flat spacetimes *Phys. Rev.* D **67** 024034
[14] Eichhorn A and Mizera A 2014 Spectral dimension in causal set quantum gravity *Class. Quantum Grav.* **31** 125007
[15] Belenchia A, Benincasa D, Marcianò A and Modesto L 2016 Spectral dimension from nonlocal dynamics on causal sets *Phys. Rev.* D **93** 044017
[16] Eichhorn A, Mizera S and Surya S 2017 Echoes of asymptotic silence in causal set quantum gravity *Class. Quantum Grav.* **34** 16LT01
[17] Carlip S 2017 Dimension and dimensional reduction in quantum gravity *Class. Quantum Grav.* **34** 193001
Abajian J and Carlip S 2018 Dimensional reduction in manifold-like causal sets *Phys. Rev.* D **97** 066007